Wang *et al.*
Natural Products and Bioprospecting (2025) 15:35
https://doi.org/10.1007/s13659-025-00516-9

Natural Products and Bioprospecting

ORIGINAL ARTICLE

Open Access

Chemical constituents of *Lycium barbarum* leaves and their anti-rheumatoid arthritis activity in vitro

Zi-Jiao Wang[1,3], Bang-Yin Tan[1,3], Yun Zhao[1,3], Chang-Bin Wang[1,3], Yun-Li Zhao[2*] and Xiao-Dong Luo[1,2*]

Abstract

Two new together with 32 known compounds were isolated from the leaves of *Lycium barbarum*. Their structures were elucidated using 1D and 2D NMR, HRESIMS, and ECD spectroscopic techniques. Compounds **1–34** were evaluated for their anti-rheumatoid arthritis activities in a lipopolysaccharide (LPS)-induced MH7A cells inflammatory model. As a result, compounds **1–3**, **6**, **8**, **10**, **14**, **17–19**, **29** and **31** inhibited the activity of lactate dehydrogenase (LDH) and nitric oxide (NO) at concentrations 20 μM. Among them, compound **1** showed the best effectiveness, with inhibition rates of 46.7% for NO and 32.8% for LDH.

Keywords *Lycium barbarum* leaves, Chemical constituents, Anti-rheumatoid arthritis

*Correspondence:
Yun-Li Zhao
zhaoyunli@ynu.edu.cn
Xiao-Dong Luo
xdluo@mail.kib.ac.cn
Full list of author information is available at the end of the article

Graphical Abstract

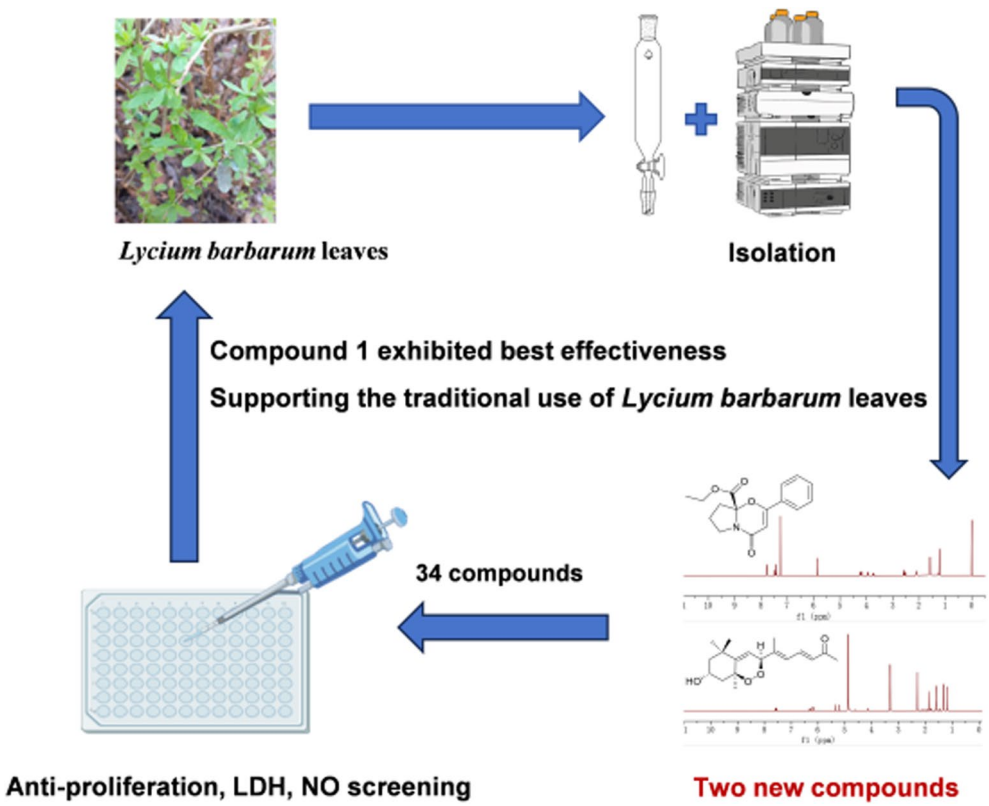

1 Introduction

Lycium barbarum L., a deciduous shrub from the Solanaceae family, is a renowned traditional plant for both medicine and food [1]. The leaves of *L. barbarum* were proven to possess various biological effects such as boosting immunity, reducing heat, alleviating rheumatic pain, quenching thirst, promoting saliva secretion, and improving eyesight [2]. In Asian countries, the leaves served as functional vegetables, commonly used in soup making, stir-frying, and as herbal teas [3].

Rheumatoid arthritis (RA), characterized by persistent inflammation and abnormal proliferation of fibroblast-like synoviocytes (FLS), was a chronic inflammatory condition that could result in joint destruction and disability [4]. The treatment of RA included glucocorticoids, disease-modifying antirheumatic drugs, nonsteroidal anti-inflammatory drugs and biologics [5]. However, these medications were expensive and came with serious side effects [6]. Then, it was essential to explore natural products for anti-RA drugs that were effective and had low toxicity. Folk applications suggested the therapeutic effects of *L. barbarum* leaves on rheumatoid arthritis, but its bioactive compounds remained unknown.

2 Results and discussion

2.1 Structural elucidation of compounds

A total of 34 compounds were isolated from leaves of *L. barbarum*, including one alkaloid (**1**), 10 terpenoids (**2–11**), 8 lignans (**12–19**), 11 phenolic acids (**20–30**), and four other compounds (**31–34**) with compounds (**1** and **2**) being newly discovered (Fig. 1). Compounds **4** and **8–19** were first isolated from *L. barbarum* leaves.

The molecular formula of lycibarin A (**1**) was assumed to be $C_{16}H_{17}NO_4$ based on HRESIMS peak at m/z 288.1221 $[M+H]^+$(calcd for $C_{16}H_{17}NO_4^+$, 288.1230) and the ^{13}C NMR spectrum, requiring 9 degrees unsaturation. Its IR spectrum displayed characteristic bands assignable to the carbonyl group (1766 cm^{-1}), and olefinic (1652 cm^{-1}). The 1D and 2D NMR spectroscopic data suggested that **1** was structurally similar to 6,7,8,8a-tetrahydro-2-phenyl-4*H*-pyrrolo[2, 1-b][1, 3] oxazin-4-one [7] with the notable difference being the presence of an additional ethyl acetate fragment in **1**.

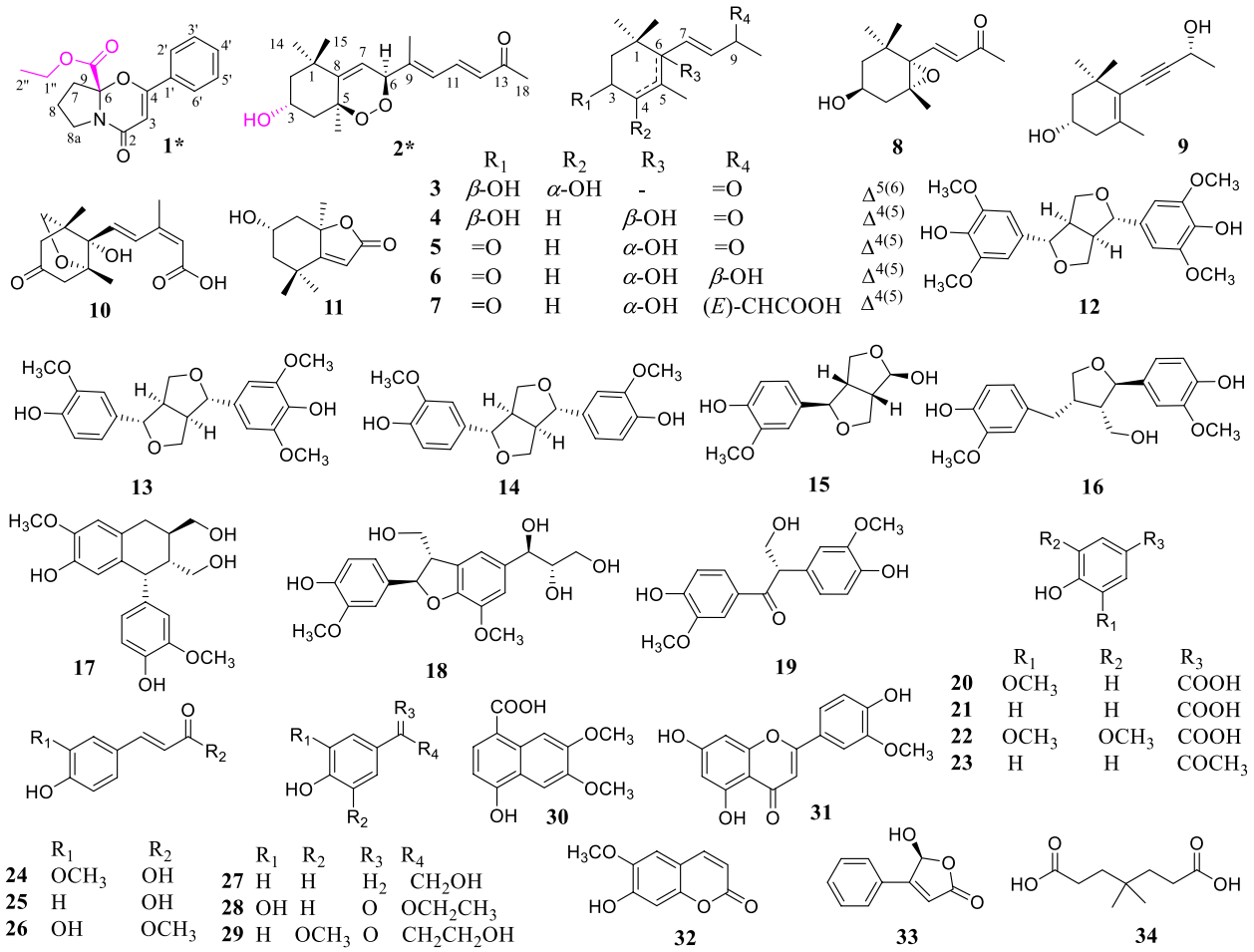

Fig. 1 Structures of **1–34**

Meanwhile, the COSY correlation of δ_H 1.23 (H-2") / 4.23 (H-1"α), and the HMBC correlation between δ_H 4.23 (H-1"α) and δ_C 170.5 (C-9) supported the presence of ethyl acetate group, while the ethyl acetate substitution at C-6 was indicated by the HMBC correlations of δ_H 2.55 (H-7) with δ_C 94.8 (C-6) and 170.5 (C-9). Then the structure of **1** was elucidated as illustrated in Fig. 2, and its chiral carbon was deduced to be 6*R* by comparing the experimental and calculated electronic circular dichroism (ECD) spectra (Fig. 3).

Compound **2** possessed a molecular formula of $C_{18}H_{26}O_4$ by its (+)-HRESIMS data at m/z 329.1698 $[M+Na]^+$ (calcd for $C_{18}H_{26}O_4Na$, 329.1723). Detailed analysis of the ^1H and ^{13}C NMR spectral data (Table 1)

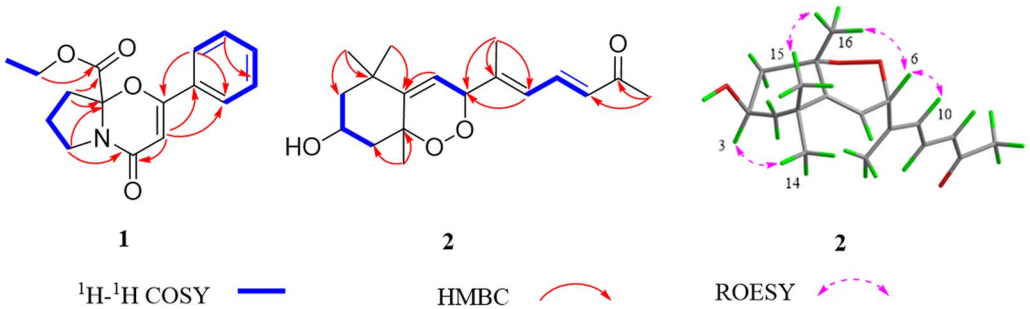

Fig. 2 The key ^1H–^1H COSY and HMBC correlations of compounds **1** and **2**

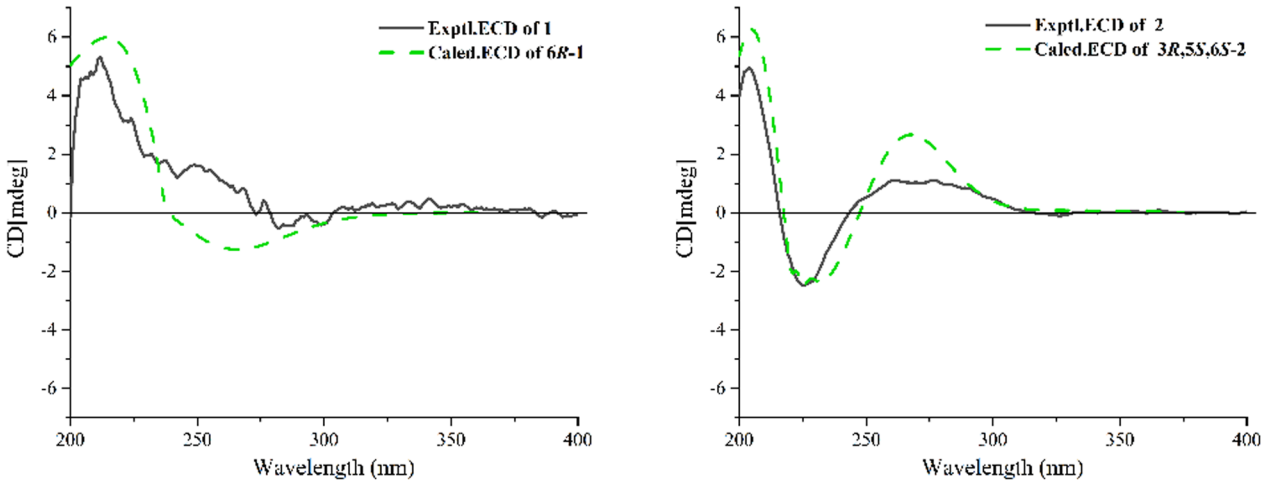

Fig. 3 The experimental and calculated ECD spectra of compounds **1** and **2**

of **2** showed high similarity to those of 5,8-endoperoxy-2,3-dihydro-*β*-apocarotene-13-one [8]. The obvious differences between the two compounds were **2** with oxymethine signal at C-3 (δ_C 68.1) instead of methylene signal (δ_C 18.6) in 5,8-endoperoxy-2,3-dihydro-*β*-apocarotene-13-one, which assumed a hydroxylated derivative of 5,8-endoperoxy-2,3-dihydro-*β*-apocarotene-13-one for **2**. Meanwhile, the COSY correlation (Fig. 2) of δ_H 4.14 (H-3) / 1.78 (H_2-2*α*) supported the hydroxyl substitution at C-3. The large coupling constant ($J_{H\text{-}11/H\text{-}12}$ = 15.4 Hz) suggested *E* configuration for $\Delta^{11,12}$, and the *E* configuration of $\Delta^{9,10}$ was supported by the NOE correlation of δ_H 5.20 (H-6) / 6.31 (H-10) in its ROESY spectrum. Additionally, NOE correlations of δ_H 5.20 (H-6) / 1.60 (H-16) and δ_H 1.60 (H-16) / 1.33 (H-15) indicated their *syn* orientation and temporarily assigned the *α*-orientation, while the *β*-configuration of H-3 was elucidated by the NOE correlation between δ_H 4.14 (H-3) / 1.18 (H_3-14) (Fig. 2). Moreover, the calculated ECD spectrum of (3*R**, 5*S**, 6*S**) configuration was matched the experimental spectrum of **2**, which assigned its absolute configuration (Fig. 3).

The 32 known compounds (**3**–**34**) were identified as (−)-(3*S*,4*S*)-eucomehastigmane B (**3**) [9], *cis*-3,6-dihydroxy-*α*-ionone (**4**) [10], (+)-dehydrovomifoliol (**5**) [11], vomifoliol (**6**) [12], *trans, trans*-abscisic acid (**7**) [13], (3*S*,5*R*,6*S*,7*E*)-5,6-epoxy-3-hydroxy-7-megastigmen-9-one (**8**) [14], 3-hydroxy-7,8-dehydro-*β*-ionol (**9**) [15], phaseic acid (**10**) [16], loliolida (**11**) [17], (+)-syringaresinol (**12**) [18], medioresinol (**13**) [19], (-)-pinoresinol (**14**) [20], (1*R**,2*R**,5*R**,6*S**)-6-(4-hydroxy-3-methoxyphenyl)-3,7-dioxabicyclo[3.3.0]octan-2-ol (**15**) [21], (+)-lariciresinol (**16**) [22], (+)-isolariciresinol (**17**) [23], meliasendanin B (**18**) [24], evofolin B (**19**) [25], vanillic acid (**20**) [26], 4-hydroxybenzoic acid (**21**) [27], syringic acid (**22**) [28], 4-hydroxyacetophenone (**23**) [29], ferulic acid (**24**) [30], *p*-coumaric acid (**25**) [31], caffeic acid methyl ester (**26**) [32], tyrosol (**27**) [33], ethyl 3,4-dihydroxybenzoate (**28**) [34], *β*-hydroxy propiovanillone (**29**) [35], 6,7-dimethoxy-4-hydroxy-1-naphthoic acid (**30**) [36], chrysoeriol (**31**) [37], scopoletin (**32**) [38], 5-hydroxy-4-phenyl-5*H*-furan-2-one (**33**) [39], 4,4-dimethylheptanedioic acid (**34**) [40].

2.2 The establishment of lipopolysaccharide (LPS)-induced MH7A inflammation model.

Previous studies showed that RA-FLS were stimulated by chemotactic factors, including IL-1β, TNF-α, and LPS [41, 42]. Additionally, LPS-induced RA-FLS displayed biological traits that were associated with RA, such as aberrant proliferation and resistance to cell death, which were similar to those of tumor cells [43]. Therefore, the immortalized RA-FLS MH7A cell line induced by LPS was utilized for in vitro studies to investigate the therapeutic effects of isolated compounds of *L. barbarum* leaves on RA. Following a 24-hour exposure to varying doses of LPS (1, 5, 10, 25, 50 and 100 μg/mL), the MTT test was used to assess the viability of the cells. As depicted in Fig. 4A, a peak cell viability of 120.8% was reached with an LPS concentration of 10 μg/mL, showing a significant difference compared to the control group ($p < 0.01$). As a result, for the subsequent stimulation, 10 μg/mL of LPS was selected.

2.3 Inhibitory effect of isolated compounds on proliferation, nitric oxide (NO) lactate dehydrogenase (LDH) production in LPS-induced MH7A cells.

Compounds were subjected to cytotoxicity testing, revealing no inhibition at a concentration of 20 μM for

Table 1 The ^{1}H NMR (600 MHz) and ^{13}C NMR (150 MHz) spectral data of compounds **1** and **2** (δ in ppm and *J* in Hz)

NO	1[a]		2[b]	
	δ_H (mult, *J*)	δ_C	δ_H (mult, *J*)	δ_C
1				34.9, s
2*α*		161.6, s	1.78, dd (14.0, 7.4)	48.7, t
2*β*			1.48, dd (14.0, 3.5)	
3	5.85, s	98.5, d	4.14, m	68.1, d
4*α*		163.7, s	2.10, dd (13.5, 3.8)	48.9, t
4*β*			1.95, dd (13.5, 4.4)	
5				89.5, s
6		94.8, s	5.20, br s	88.6, d
7	2.55, m	36.8, t	5.35, br s	120.2, d
8	2.10, m	21.2, t		156.3, s
8a*α*	3.93, dt (11.0, 7.0)	45.2, t		
8a*β*	3.73, dt (11.0, 7.0)	-		
9	-	170.5, s		151.2 s
10			6.31, d (11.4)	125.3, d
11			7.57, dd (15.4, 11.4)	141.2, d
12			6.19, d (15.4)	131.5, d
13				201.8, s
14			1.18, s	31.9, q
15			1.33, s	29.7, q
16			1.60 s	29.6, q
17			1.86, s	13.5, q
18			2.30, s	27.4, q
1′	-	131.5, s		
2′/6′	7.78, d (7.6)	127.2, d		
3′/5′	7.44, t (7.6)	128.6, d		
4′	7.48, t (7.6)	131.4, d		
1″*α*	4.23, dq (10.8, 7.2)	62.4, t		
1″*β*	4.18, dq (10.8, 7.2)			
2″	1.23, t (7.2)	14.0, q		

a: in $CDCl_3$

b: in CD_3OD

all (Fig. 4B–C). Furthermore, compounds **1–4**, **6**, **8–14**, **16–21**, **23–24**, and **29–33** demonstrated substantial inhibitory effects on the proliferation bioactivity of LPS-induced MH7A cells ($p < 0.05/0.01$, Table S1). It was worth mentioning that the cell viabilities of compounds **1** and **2** were 112.91% and 116.47%, respectively (Fig. 5A–B). Synovial cells were considered the primary producers of NO in RA. Synovial fibroblasts were induced by pro-inflammatory cytokines to produce NO, thereby enhancing the production of inflammation [44]. LDH, a cytoplasmatic enzyme, present in essentially all organ systems is thought to be released only after cell death and local inflammation of cells may be a potential source of elevation of LDH [45]. As cells underwent proptosis, pores formed within them, resulting in an elevation of LDH levels [46]. Stimulation with LPS on MH7A cells led to elevated levels of NO and LDH production by MH7A cells compared to the control group, whereas compounds **1–3**, **6**, **8**, **10–12**, **14**, **16–19**, **21**, **29** and **31** displayed inhibitory effects on NO ($p < 0.05/0.01$, Table S2), with compounds **1–3**, **6**, **8–10**, **14**, **17–19, 29** and **31–32** also showing inhibitory effects on LDH release ($p < 0.05/0.01$, **Table S3**). The compounds **1–3**, **6**, **8**, **10**, **14**, **17–19**, **29** and **31** exhibited effectiveness on LDH and NO indicators ($p < 0.05/0.01$, Table S4). Among them, compounds **1** and **2** exhibited good inhibitory activity on the two indicators, NO inhibition rates were 46.7% and 26.8% respectively, and LDH inhibition rates were 32.8% and 22.8% respectively (Fig. 5C–F).

3 Experimental

3.1 General experimental procedures

NMR, HRESIMS, UV, and IR spectra were obtained following the previously described methods [47].

3.2 Plant material

The origin of the plant material is detailed in the **Plant Material** section of Supplementary Material.

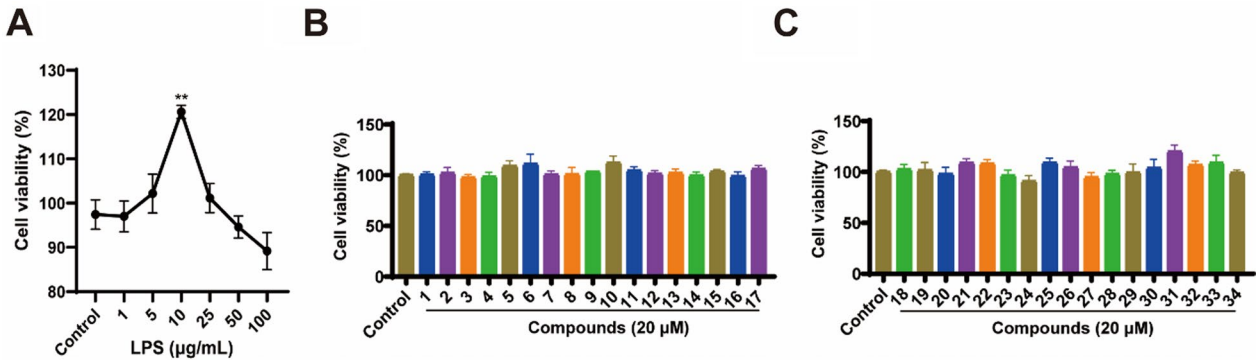

Fig. 4 **A** Cell viability of MH7A cells under stimulation of different concentrations of LPS. **B-C** The cell viability of compounds on MH7A cells. Compared with the control group, ** $p < 0.01$

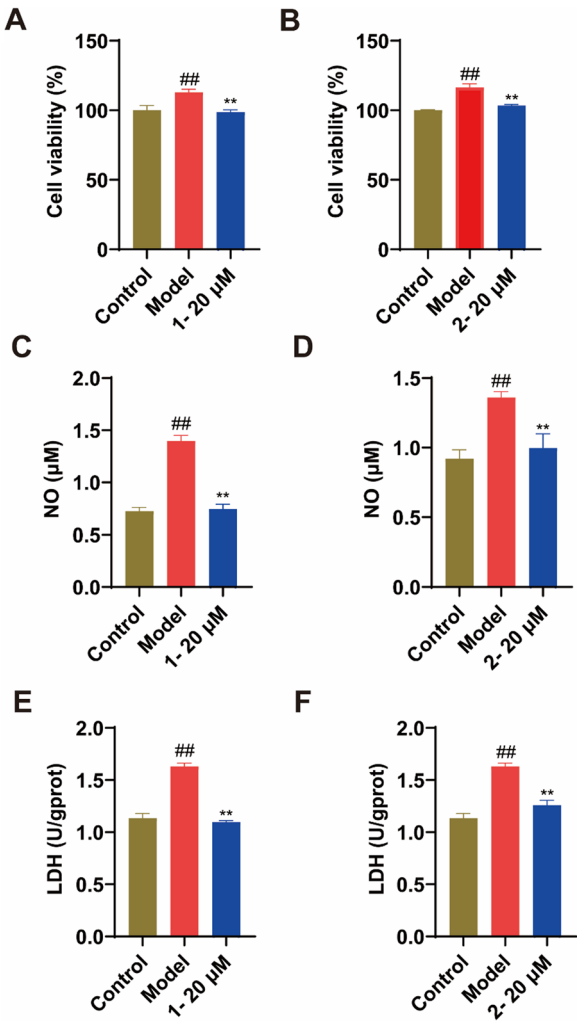

Fig. 5 The cell viabilities of compounds **1** and **2** on MH7A by LPS induction (**A**-**B**). The effect of compounds **1** and **2** on the production of NO (**C**-**D**) and the release of LDH (**E**–**F**) in LPS-induced MH7A. Compared with the control group, ## $p < 0.01$; compared with the model group, ** $p < 0.01$, respectively

3.3 Extraction and purification

The detailed procedures for extraction and isolation can be found in the **Extraction and purification** section of Supplementary Material.

Lycibarin A (**1**). white powder; $[\alpha]_D^{22}$−72.9 (0.073, MeOH); UV (MeOH) λ_{max} (log ε): 292 (3.80) nm; ECD (MeOH) λ_{max} ($\Delta\varepsilon$) 210 (+14.60), 245 (−8.78) nm; IR ν_{max} 1746, 1652, 1433, 1047, 693 cm^{-1}; ^1H NMR and ^{13}C NMR data see Table 1. HRESIMS *m/z* 288.1221$[M+H]^+$ (calcd. for $C_{16}H_{18}NO_4$, 288.1230).

Lycibarin B (**2**). white power; $[\alpha]_D^{22}$−57.2 (0.056, MeOH); UV (MeOH) λ_{max} (log ε): 288 (3.54) nm; ECD (MeOH) λ_{max} ($\Delta\varepsilon$) 209 (-1.08), 252 (+0.32) nm; IR ν_{max} 3434, 1713, 1630, 1459, 1384, 1149, 1081 cm^{-1}; ^1H and ^{13}C NMR data see Table 1; HRESIMS *m/z* 329.1698$[M+Na]^+$(calcd. for $C_{18}H_{26}O_4Na$, 329.1723).

3.4 Cell culture

MH7A (RA-FLS) cell line was obtained from Jennio Biotech Co., Ltd. (Guangzhou, China) and cultured at 37℃ with 5% CO_2 in DMEM (Gbico, USA) supplemented with 10% FBS (Procell, China), 100 U/mL penicillin, and 100 μg/mL streptomycin.

3.5 LPS-induced MH7A cells inflammation model

The MTT test was used to assess the cell viability of LPS on MH7A cells [48]. Each well was initially seeded with 1.5×10^4 cells, which were then spilt into control and LPS groups. The cells were incubated for 24 h before being treated to different doses of LPS (1, 5, 10, 25, 50 and 100 μg/mL) for another 24 h. Subsequently, 100 μL of MTT (Aladdin, Shanghai, China) was added at 0.5 mg/mL concentration and continued for 4 h. The supernatant was sucked out, and 100 μL DMSO was added to each well, followed by a 10-min incubation. The absorbance cell medium was measured at 490 nm using microplate reader (Molecular Devices, Shanghai, China).

3.6 Cell viability assay

In short, 100 μL of MH7A cell suspension (1.5×10^5 cells/mL) was added to a 96-well plate. Upon reaching 70%-80% confluence, the cells were exposed to the compounds at a 20 μM concentration for 24 h.

3.7 Inhibition of compounds on LPS-induced MH7A cells proliferation

According to the results of viability, MH7A cells were seeded in 96-cell plates for 24 h incubation and divided into control, LPS (model group), LPS and different compounds (20 μM). All groups, except for the control, were stimulated with LPS for 24 h. The steps that followed for evaluating cell viability were in accordance with the instructions outlined in previous section [49].

3.8 NO assay

After being planted in 96-well plates at a density of 1.5×10^4 cells per cell, MH7A cells were incubated for 24 h. Following this, the cells were stimulated with LPS (10 μg/mL) and treated with the tested compounds at a concentration of 20 μM. A microplate reader (Shanghai, Molecular Devices, China) was used to quantify NO at 540 nm after 50 μL of the supernatant from each well as moved to a new 96-well plate following a 24-hour incubation period [50].

3.9 LDH measurement

MH7A cells were seeded in 6-well plates and incubated with LPS and the tested compounds for 24 h. Removed the cell culture supernatant, collected the cells, and then performed the measurement according to the LDH assay kit [49].

Supplementary Information

The online version contains supplementary material available at https://doi.org/10.1007/s13659-025-00516-9.

Additional file 1. The spectral data of known compounds **3-34**; 1D and 2D NMR, HRESIMS, IR, CD and UV spectra of new compounds **1**-**2**; the ECD calculation details of new compounds; inhibitory effects of 34 compounds on proliferation, NO, LDH production in LPS-induced MH7A cells.

Author contributions

Xiao-Dong Luo conceptualized the projects, revised manuscript and provided financial support. Yun-Li Zhao supervised the experiment, revised the manuscript. Zi-Jiao Wang, Bang-Yin Tan, Yun Zhao, Chang-Bin Wang finished the isolation and identification studies. Zi-Jiao Wang implemented the anti-rheumatoid arthritis studies. Zi-Jiao Wang wrote the original draft. All authors approved the final version of the manuscript.

Funding

This research received financial backing from the High-level Talent Promotion and Training Project of Kunming (grant number 2022SCP003), Project of Yunnan Characteristic Plant Screening and R&D Service CXO Platform (grant numbers 2022YKZY001, 2023YKZY001, 2023YKZY004), Yunnan Provincial Science and Technology Project at Southwest United Graduate School (No. 202302AP370006), the Major Science and Technology Project of Yunnan Province (202302AA310013), and the Guiding Funds of the Central Government for Supporting the Development of Local Science and Technology (202407AD110002). Special thanks are extended to the Analysis and Measurement Center of Kunming Institute of Botany for their technical assistance.

Data availability

The data supporting the results of this study can be obtained from the corresponding author on reasonable request.

Declarations

Competing interests

According to policy as well as my moral obligation, the corresponding author Xiao-Dong Luo is the Executive Editor-in-Chief of Natural Products and Bioprospecting. This submission represents genuine academic work and is not influenced by editorial role of Prof. Luo. To ensure impartiality and adherence to publishing ethics, the following measures have been taken: (1) Full Recusal from Editorial Handling. (2) Transparency in Peer Review.

Author details

[1]State Key Laboratory of Phytochemistry and Plant Resources in West China, Kunming Institute of Botany, Chinese Academy of Sciences, Kunming 650201, P. R. China. [2]Yunnan Characteristic Plant Extraction Laboratory Co. Ltd, Key Laboratory of Medicinal Chemistry for Natural Resource, Ministry of Education, Yunnan Key Laboratory of Research and Development for Natural Products, School of Pharmacy, School of Chemical Science and Technology, Yunnan University, Southwest United Graduate School, Kunming 650091, P. R. China. [3]University of Chinese Academy of Sciences, Beijing 100049, P. R. China.

Received: 27 March 2025 Accepted: 21 April 2025
Published online: 30 May 2025

References

1. Zhang L, Li Y, Yan Q, Ning Y, Wang Y, Liu K, Qiang Y, Ma X, Sun X. Establishment of high performance liquid chromatographic fingerprint and determination of 4 kinds of phenolic acid bioactive substances of fruitless *Lycium barbarum* leaves from Ningxia at different harvesting periods. Heliyon. 2024;10: e24614.
2. Zhang B, Wang M, Wang C, Yu T, Wu Q, Li Y, Lv Z, Fan J, Wang L, Zhang B. Endogenous calcium attenuates the immunomodulatory activity of a polysaccharide from *Lycium barbarum* L. leaves by altering the global molecular conformation. Int J Biol Macromol. 2019;123:182–8.
3. Gong G, Fan J, Sun Y, Wu Y, Liu Y, Sun W, Zhang Y, Wang Z. Isolation, structural characterization, and antioxidativity of polysaccharide LBLP5-A from *Lycium barbarum* leaves. Process Biochem. 2016;5:314–24.
4. Li Y, Li A, Xing Y, Jiang Y, Pei H, He Z, Li J, Zhao Y, Shi K, Zong Y, Du R. Gastrodin targets the system Xc-/GPX4 axis to inhibit abnormal proliferation of fibroblast-like synoviocytes and improve rheumatoid arthritis. Phytomedicine. 2025;139: 156493.
5. Pan L, Zhou T, Maimaiti K, Xu H, Ma G. Anti-rheumatoid arthritis effects of Caragana acanthophylla Kom. on collagen-induced arthritis and the anti-inflammatory activity of polyphenols as main active components. J Ethnopharmacol. 2025;346:119637.
6. Jing R, Ban Y, Xu W, Nian H, Guo Y, Geng Y, Zang Y, Zheng C. Therapeutic effects of the total lignans from *Vitex Negundo* seeds on collagen-induced arthritis in rats. Phytomedicine. 2019;58: 152825.
7. Wessig P, Schwarz J, Lindemann U, Holthausen MC. Photochemical synthesis of 3, 4-dihydro-2H-1, 3-oxazin-4-ones. Synthesis. 2001;112:1258–62.
8. Hu X, White KM, Jacobsen NE, Mangelsdorf DJ, Canfield LM. Inhibition of growth and cholesterol synthesis in breast cancer cells by oxidation products of *β*-carotene. J Nutr Biochem. 1998;6:567–74.
9. Yan J, Shi X, Donkor PO, Zhu H, Gao X, Ding L, Qiu F. Nine pairs of megastigmane enantiomers from the leaves of *Eucommia ulmoides* Oliver. J Nat Med. 2017;71:780–90.
10. Serra S, Barakat A, Fuganti C. Chemoenzymatic resolution of *cis*- and *trans*-3,6-dihydroxy-*α*-ionone. Synthesis of the enantiomeric forms of dehydrovomifoliol and 8,9-dehydrotheaspirone. Tetrahedron Asymmetry. 2007;8:2573–80.
11. Jin Q, Lee C, Lee JW, Yeon ET, Lee D, Han SB, Hong JT, Kim Y, Lee MK, Hwang BY. 2-Phenoxychromones and prenylflavonoids from *Epimedium koreanum* and their inhibitory effects on LPS-induced nitric oxide and interleukin-1*β* production. J Nat Prod. 2014;77:1724–8.
12. Fan XZ, Song JQ, Shi XY, Zhou JF, Yuan RJ, Liu T, Kong XQ, Huang YS, Zhang LJ, Liao HB. New sesquiterpenoids with neuroprotective effects *in vitro* and *in vivo* from the *Picrasma chinensis*. Fitoterapia. 2024;175: 105908.
13. Zheng JX, Zheng Y, Zhi H, Dai Y, Wang NL, Fang YX, Du ZY, Zhang K, Wu LY, Fan M. γ-Lactone derivatives and terpenoids from *Selaginella uncinata*. Chem Nat Compd. 2014;50:366–72.
14. D'Abrosca B, Della GM, Fiorentino A, Monaco P, Oriano P, Temussi F. Structure elucidation and phytotoxicity of C13 nor-isoprenoids from *Cestrum parqui*. Phytochemistry. 2004;65:497–505.
15. Luo Y, Li XZ, Xiang B, Luo Q, Liu JW, Yan YM, Sun Q, Cheng YX. Cytotoxic and renoprotective diterpenoids from *Clerodendranthus spicatus*. Fitoterapia. 2018;125:135–40.
16. Shi YS, Liu YB, Ma SG, Li Y, Qu J, Li L, Yuan SP, Hou Q, Li YH, Jiang JD, Yu SS. Bioactive sesquiterpenes and lignans from the fruits of *Xanthium sibiricum*. J Nat Prod. 2015;78:1526–35.
17. Yang C, Mao H, Qi X, Zhang Y, Cao Y, Tao L, Dong X, Zhang Y. Chemical constituents from the stems of *Ostodes paniculata* Bl. (Euphorbiaceae). Biochem Syst Ecol. 2024;113:104807.
18. Wang W, Jiang L, Zhu Y, Mei L, Tao Y, Liu Z. Bioactivity-guided isolation of cyclooxygenase-2 inhibitors from *Saussurea obvallata* (DC.) Edgew. using affinity solid phase extraction assay. J Ethnopharmacol. 2022;284:114785.
19. Ramabulana T, Scheepers LM, Moodley T, Maharaj VJ, Stander A, Gama N, Ferreira D, Sonopo MS, Selepe MA. Bioactive lignans from *Hypoestes aristata*. J Nat Prod. 2020;83:2483–9.
20. Zhou H, Ren J, Li Z. Antibacterial activity and mechanism of pinoresinol from *Cinnamomum camphora* leaves against food-related bacteria. Food Control. 2017;79:192–9.
21. Li BB, Li JL, Li N, Qi SZ, Lee HS, Zhang L, Xing SS, Tuo ZD, Cui L. Diacylglycerol acyltransferase 1 (DGAT1) inhibition by furofuran lignans from stems of *Acanthopanax senticosus*. Arch Pharm Res. 2017;40:1271–7.

22. Bajpai VK, Shukla S, Paek WK, Lim J, Kumar P, Kumar P, Na M. Efficacy of (+)-lariciresinol to control bacterial growth of *Staphylococcus aureus* and *Escherichia coli* O157:H7. Front Microbiol. 2017;8:804.
23. Huang Y, Hou P, Pan L, Li J, Liang X, Ren C, Peng L, Gan C, Xu W, Yang R, Li J, Guan X. Lignans and phenols with potential anti-inflammatory effect from the stems of *Mallotus paxii* Pamp. Fitoterapia. 2024;179: 106253.
24. Wang L, Li F, Yang CY, Khan AA, Liu X, Wang MK. Neolignans, lignans and glycoside from the fruits of *Melia toosendan*. Fitoterapia. 2014;99:92–8.
25. Wang J, Zhang X, Yu J, Du J, Wu X, Chen L, Wang R, Wu Y, Li Y. Constituents of the fruits of *Rubus chingii* Hu and their neuroprotective effects on human neuroblastoma SH-SY5Y cells. Food Res Int. 2023;173: 113255.
26. Zhou H, Jian R, Kang J, Huang X, Li Y, Zhuang C, Yang F, Zhang L, Fan X, Wu T, Wu X. Anti-inflammatory effects of caper (*Capparis spinosa* L.) fruit aqueous extract and the isolation of main phytochemicals. J Agric Food Chem. 2010;58:12717–21.
27. Oh CH, Kim NS, Yang JH, Lee H, Yang S, Park S, So UK, Bae JB, Eun JS, Jeon H, Lim JP, Kwon J, Kim YS, Shin TY, Kim DK. Effects of isolated compounds from *Catalpa ovata* on the T Cell-mediated immune responses and proliferation of leukemic cells. Arch Pharm Res. 2010;33:545–50.
28. Nukulkit S, Nalinratana N, Aree T, Suriya U, Suttisri R, Nuengchamnong N, Chang HS, Chansriniyom C. Maeruines A–E, elusive indole alkaloids from stems of *Maerua siamensis* and their inhibitory effects on cyclooxygenases and HT-29 colorectal cancer cell proliferation. Phytochemistry. 2025;22: 114291.
29. Kang U, Park J, Han AR, Woo MH, Lee JH, Lee SK, Chang TS, Woo HA, Seo EK. Identification of cytoprotective constituents of the flower buds of *Tussilago farfara* against glucose oxidase-induced oxidative stress in mouse fibroblast NIH3T3 cells and human keratinocyte HaCaT cells. Arch Pharm Res. 2016;39:474–80.
30. Xiao H, Parkin K. Isolation and identification of phase II enzyme-inducing agents from nonpolar extracts of green onion (*Allium* Spp.). J Agric Food Chem. 2006;54:8417–24.
31. Stefani T, Romo-Mancillas A, Carrizales-Castillo JJJ, Arredondo-Espinoza E, Ramírez-Estrada K, Alcantar-Rosales VM, González-Maya L, Sánchez-Carranza JN, Balderas-Renterías I, Camacho-Corona MDR. Cytotoxic fractions from *Hechtia glomerata* extracts and *p*-coumaric acid as MAPK inhibitors. Molecules. 2021;26:1096.
32. Chang SW, Kim KH, Lee IK, Choi SU, Ryu SY, Lee KR. Phytochemical constituents of *Bistorta manshuriensis*. Nat Prod Sci. 2009;15:234–40.
33. Abo-Qotb SMS, Hassanein AMM, Desoukey SY, Wanas AS, Tawfik HM, Orabi MAA. In vivo anti-inflammatory and hepatoprotective activities of Orobanche crenata (Forssk) aerial parts in relation to its phytomolecules. Nat Prod Res. 2022;36:1067–72.
34. Reis B, Martins M, Barreto B, Milhazes N, Garrido EM, Silva P, Garrido J, Borges F. Structure–property–activity relationship of phenolic acids and derivatives. protocatechuic acid alkyl esters. J Agric Food Chem. 2010;58:6986–93.
35. Luo JR, Jiang HE, Zhao YX, Zhou J, Qian JF. Components of the heartwood of *Populus euphratica* from an ancient tomb. Chem Nat Compd. 2008;44:6–9.
36. Zhang YW, Sun WX, Li X, Zhao CC, Meng DL, Li N. Two new compounds from *Helichrysum arenarium* (L.). J Asian Nat Prod Res. 2009;11:289–93.
37. Wang Y, Zhang H, Su X, Yang H, Sun W. Flavonoids and phenolic compounds of *Petrosimonia sibirica*. Chem Nat Compd. 2016;52:482–3.
38. Wu Q, Zou L, Yang XW, Fu DX. Novel sesquiterpene and coumarin constituents from the whole herbs of *Crossostephium chinense*. J Asian Nat Prod Res. 2009;11:85–90.
39. Wang W, Yang H, Chen Y. Constituents of *Microsorum insigne*. Chem Nat Compd. 2017;53:789–90.
40. Xiao BK, Yang JY, Liu YR, Dong JX, Huang RQ. Chemical constituents of *Pittosporum illicioides*. Chem Nat Compd. 2015;51:1126–9.
41. Luo S, Li H, Liu J, Xie X, Wan Z, Wang Y, Zhao Z, Wu X, Li X, Yang M, Li X. Andrographolide ameliorates oxidative stress, inflammation and histological outcome in complete freund's adjuvant-induced arthritis. Chem-Biol Interact. 2020;319: 108984.
42. Ma X, Yang Y, Li H, Luo Z, Wang Q, Yao X, Tang F, Huang Y, Ling Y, Ma W. Periplogenin inhibits pyroptosis of fibroblastic synoviocytes in rheumatoid arthritis through the NLRP3/Caspase-1/GSDMD signaling pathway. Int Immunopharmacol. 2024;133: 112041.
43. Tong S, Liu J, Zhang C. Platelet-rich plasma inhibits inflammatory factors and represses rheumatoid fibroblast-like synoviocytes in rheumatoid arthritis. Clin Exp Med. 2017;17:441–9.
44. Mo X, Chen J, Wang X, Pan Z, Ke Y, Zhou Z, Xie J, Lv G, Luo X. Krüppel-like factor 4 regulates the expression of inducible nitric oxide synthase induced by TNF-α in human fibroblast-like synoviocyte MH7A cells. Mol Cell Biochem. 2018;438:77–84.
45. Akinloye OA, Alagbe OA, Ugbaja RN, Omotainse SO. Evaluation of the modulatory effects of Piper guineense leaves and seeds on egg albumin-induced inflammation in experimental rat models. J Ethnopharmacol. 2020;255: 112762.
46. Zhang Y, Cai X, Wang B, Zhang B, Xu Y. Exploring the molecular mechanisms of the involvement of GZMB-Caspase-3-GSDME pathway in the progression of rheumatoid arthritis. Mol Immunol. 2023;161:82–90.
47. Zhu PF, Dai Z, Wang B, Wei X, Yu HF, Yan ZR, Zhao XD, Liu YP, Luo XD. The anticancer activities phenolic amides from the stem of *Lycium barbarum*. Natur Prod & Bioprosp. 2017;7:421–31.
48. Chen YC, Liu YY, Chen L, Tang DM, Zhao Y, Luo XD. Antimelanogenic effect of isoquinoline alkaloids from *Plumula nelumbinis*. J Agric Food Chem. 2023;71:16090–101.
49. Li C, Tang S, Hu T, Zhou C, Chen Y, Hu Z, Pan J, Chen J, Wang Y. Exploring the potential mechanism of action of Wutou-Guizhi decoction in the treatment of rheumatoid arthritis through network pharmacology analysis. Comput Biol Chem. 2025;115: 108314.
50. Chen S, Tian CB, Bai LY, He XC, Lu QY, Zhao YL, Luo XD. Thrombosis inhibited by *Corydalis decumbens* through regulating PI3K-Akt pathway. J Ethnopharmacol. 2024;329: 118177.

Publisher's Note